

Impact of equatorial Kelvin waves on aggregations of sardinellas (*Sardinella* spp.) in Angolan waters.

Marek Ostrowski

High yields of pelagic fish in Angolan tropical waters are associated with seasonal upwelling. The Angolan upwelling is forced by a large-scale eastward tilt of the main thermocline in the tropical Atlantic. Near the coast, the nutrient-rich layer of central water elevates to less than a 20 m depth. Enrichment and high productivity occurs in the absence of upwelling favourable wind, forced by low energetic processes such as lateral mixing or internal waves. Under these conditions, small pelagic fish (mainly *Sardinella aurita* and *S. maderensis*) forms highly contiguous aggregations aligned along topographic features and close inshore. Twice a year, upwelling is interrupted by a strong El Niño-like poleward current, associated to coastally-trapped Kelvin waves remotely forced in the western tropical Atlantic. The thermocline becomes depressed to 40-60 meters while the surface layer is intruded by an oligotrophic layer of warm and low salinity water of equatorial origin. Downwelling conditions dominate along the entire coast. However, the downwelling is visibly stronger to the north of Luanda (latitude 8° 50'S) where the sea level rises and thermocline depresses additionally due to partial blocking of the poleward flow by the westward offset of the continental shelf located just south of the city. Under these conditions distribution patterns of sardinella changes significantly. They appear to use the poleward current as the transport mechanism to avoid harsh conditions. Few fish are detected to the north of Luanda; their largest aggregations are shifted further the south. Individual schools or school clusters are typically larger to those observed during upwelling seasons. However, at larger scales fish distributions are not contiguous and not related to oceanographic or bathymetric gradients.

Keywords: Tropical ecosystem, Kelvin waves, pelagic fish aggregations

Contact author:

Marek Ostrowski: Institute of Marine Research, P.O. Box 1870

5817 Bergen, Norway [tel: + 47 55 23 86 23]

e-mail: mareko@imr.no

1. Introduction

The coastal ocean off Angola supports large pelagic fisheries of sardinellas, *Sardinella aurita* and *S. maderensis*. The main area of concentration of these species is located in the northern and central shelf regions between 6° and 13°S (FAO, 2000). Sardinella stock exhibits a strong seasonal migration pattern. According to the acoustic surveys with the Norwegian vessel RV *Dr. Fridtjof Nansen*, higher biomass is observed in the north during austral winters and in the south of Luanda in summers (FAO, 2000). These results are supported by historical reports on sardinella catches in also showing that more fish was captured in the northern Angola during winters than in summers (FAO, 1979). A review of seasonal migrations of sardinella in the southeastern Atlantic is given by Boley and Fréon (1980). Off Congo, spawning of *Sardinella aurita* occurs twice seasonally coinciding with two cold seasons, the main one from February to September and the secondary in January. Migrations of adults exhibit two cycles annually with the southward and northward movements coinciding with the warm and cold season, respectively (Fig. 5; Boley and Fréon, 1980). The first, large-scale cycle occurs during the first half of the year with fish migrating southwards in February-March-April towards the southern Angola and returning towards Congo in June-July-August. The second, weaker cycle is confined to Congo and the northern Angola with the southward migration in October-November and northward return in December-January.

The seasonality in distributions of small pelagic fish off Angola matches the annual cycle of coastal oceanography. Hydrographic regimes alternate seasonally from intrusions periods of warm and low salinity equatorial water during austral summers to upwelling seasons in winters (Berrit and Dias, 1977; Strømme et al., 1986; Bianchi, 1992). In contrast to the Benguela Upwelling area (Shannon and Nelson, 1996), the oceanographic variability over the Angola's continental shelf to the north of 13°S is controlled via remotely forced free coastal Kelvin waves; correlation to local wind conditions is poor (Berrit, 1976; Picaut, 1983; Lazar et al., 2006). An oceanic teleconnection mechanism linking forcing in the western Atlantic to variability in the eastern tropical Atlantic was proposed by Moore et al. (1978). In the western side of the basin, a semiannual cycle dominates variation of strong SE winds. The seasonal change of this wind controls the depth of the thermocline along the African coast (Philander and Pacanowski, 1986). The wind relaxes in the beginning of the year and this relaxation generates baroclinic downwelling Kelvin waves (high pressure cells) that propagate

eastward along the equator. In May-June the trade wind in the western Atlantic strengthens sending upwelling Kelvin waves (low-pressure cells). A second similar cycle takes place during the second half of the year (September to January). Upon reaching the African continent boundary these waves are transformed into coastally trapped waves which propagate towards the poles. These waves control the height of the thermocline and direction of geostrophic current near the coast: downwelling waves depress the thermocline and force a poleward flow while the upwelling waves rise the thermocline and force an equatorial flow (Bakun, 1996). Schouten et al. (2005) identified propagation of coastally-trapped Kelvin waves along the Angola's coast in remotely-sensed altimetry. According to their study, seasonal downwelling (high pressure cells) arrive at the Angolan coast in February-March and in October-November. The opposite phase, upwelling Kelvin waves (low-pressure cells) peak at the Angolan coast in June-July, coinciding with the upwelling season. Amplitude of these seasonal propagations decays rapidly south of 13°S (Lazar et al., 2006). Rouault and Lutjeharms (2003) monitored seasonal propagations of Kelvin wave-like features along the Angolan coast from remotely-sensed SST data. Using a model, Florenchie et al.(2003) demonstrated that coastally-trapped downwelling Kelvin waves sourced extreme warm events in northern Benguela, known as Benguela Niños, observed on decadal time scales (Shannon et al., 1986). In the follow-up work, Florenchie et al.(2004) showed that in the Angola-Benguela area located between 10° and 20°S, impacts of remote forcing from the western Atlantic are not only limited to extreme events, but are the main factor controlling development of warm and cold SST anomalies on interannual timescales.

This paper combines analyses of sea surface height (SSH) from satellite derived altimetry with *in situ* oceanographic and fisheries data from surveys carried out systematically during the peaks of the high and low SSH seasons in Angolan waters between 1994 and 1998. The aim is to investigate association of seasonal trends in sardinella biomass to variability of coastally-trapped oceanic waves propagating over the Angolan shelf, evidenced by satellite altimetry. The analysis presented is in this paper based necessarily on few simplifications. Only environmental factors are assumed to influence the abundance. Fishing pressure is thought constant over the entire investigation period 1994-1998, a view justified by results of the regional stock assessment work (FAO, 2000). Difference in ecological preferences of *Sardinella aurita* and *S. maderensis* are not considered. Binet et al. (2001) has demonstrated how different origins of anomalous events in the eastern Atlantic force a separation and different availability of these two species to fisheries. However, since acoustic biomass data

used in this paper (see Section 2) make no distinction between these species, we are only able to report the result for the combined stock of *Sardinella spp.* only.

2. The study area

This study pertains to the tropical sector of Angola's coastline located between 7° and 14°S, see Figure 1. A 1 km digital terrain model of the coastal bathymetry based acoustic data collected with *Dr. F. Nansen* 1994-2006 is shown in Figure 1. Four major areas exhibiting roughly uniform shelf slopes may be identified. The Ambriz Upwelling Area (AUA) runs along the incision of the continental slope extending from N'Zeto to Luanda. The shelf width is about 45 km with the shelf break at a depth of 120-130 m. Rio Longo Upwelling Area (RLUA) located between Rio Longo and Porto Amboim, has a similar topographic characterization, but is separated from AUA by the shelf discontinuity located just south of Luanda. Located further south is Lobito Shelf Area (LSA), separated from the RLUA by a large incision of the continental shelf between Porto Amboim and Quicombo. The width of the shelf to the south of this discontinuity decreases monotonically to vanish altogether off Baía Farta (12°35'S). Located at the southern extremity of the study region is North Angola-Benguela Area (NABA). It runs along a very steep section of the coastline where the continental shelf is absent and the coastal plane descends immediately towards the continental slope. The largest concentrations of pelagic fish along the Angolan coast are typically found in the two main upwelling areas, the AUA and RLUA.

3. Materials and methods

The *in situ* data reported in this paper were collected within the framework of a Norwegian development and capacity building program committed to investigations of fisheries resources in developing countries (The Dr. Fridtjof Nansen Programme; Sætelsdal et al., 1999). Off Angola, fish census surveys have been carried out since 1985 (Strømme et al., 1986; Strømme and Sætelsdal, 1991). In 1994 the program's new vessel started monitoring surveys off Angola. These surveys are continued until today. In this paper, we focus on data from acoustic surveys from 1994 to 1998, since during this period acoustic estimates of pelagic fish were conducted out twice a year during austral summer (March) and in

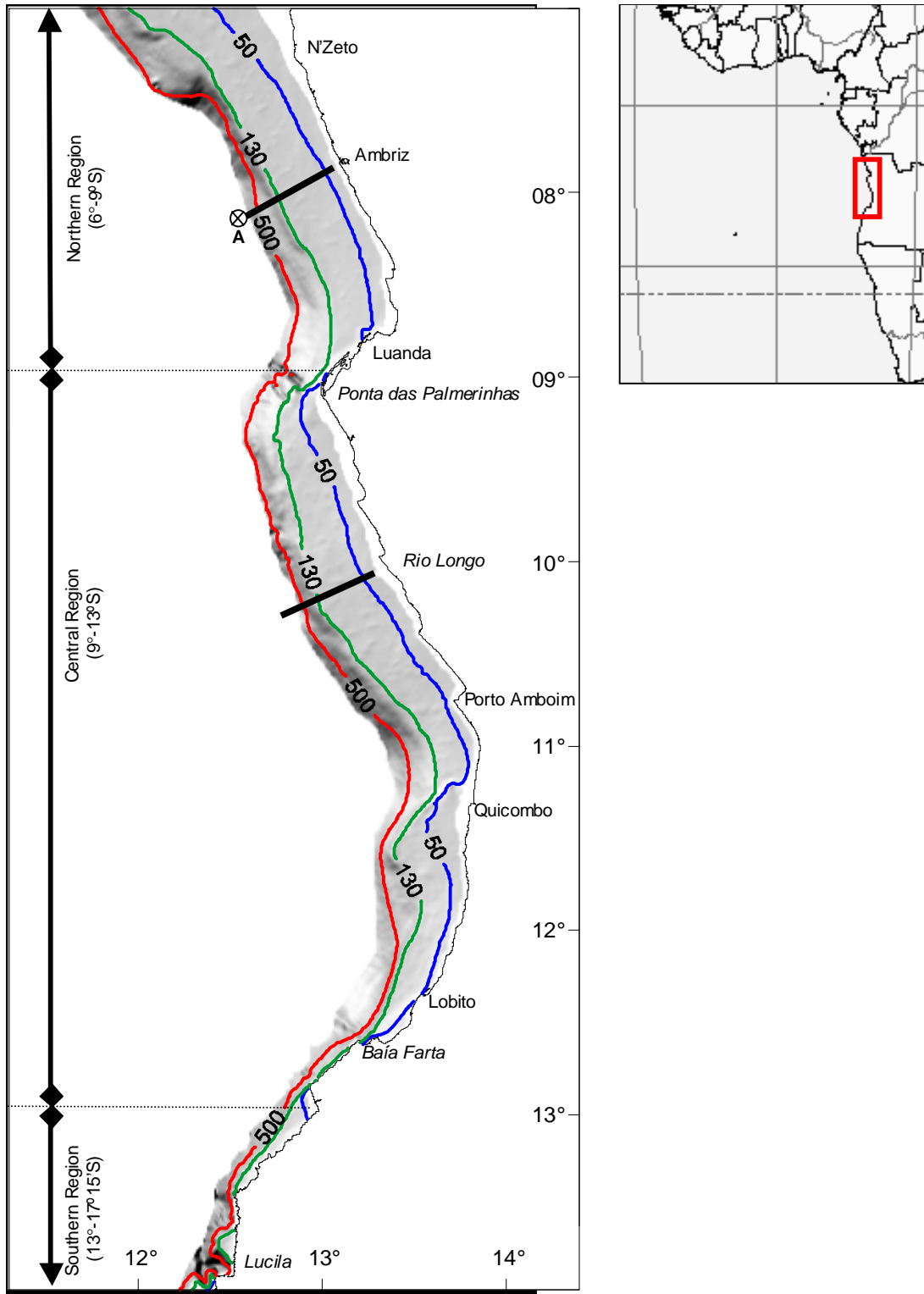


Figure 1. The study area in the tropical sector of Angola shown on top of a digital bathymetry derived from *Dr. F Nansen* acoustic data. The borders between the regions used in biomass estimates shown in the left. The insert depicts location of the survey area along the Africa's coast.

winter (August-September), thus coinciding with the first semiannual peaks of the high and low SSH seasons, respectively.

Acoustic data were collected using Simrad EK500 split-beam scientific echo sounder (Kongsberg Simrad AS, Kongsberg, Norway) fitted with four transducers operating at 18, 38, 120 and 200 kHz. The echo sounder calibration occurred during surveys, using a standard procedure with a sphere (Foote et al., 1987). The data were scrutinized using the BEI echo integrator system (Foote et al., 1992). Acoustic area backscattering coefficient (S_A ; MacLennan et al., 2002) was allocated to a predefined group of species over each elementary sampling distance unit (EDSU; of 1 or 5 nautical miles) based on echotrace characteristics and targeted trawling. Conversion from acoustic backscattering units to biomass estimates by region for each species group separately was performed according to a standard procedure described in FAO (2000). Co-occurring *Sardinella aurita* and *S. maderensis* could not be separated by this method and therefore only the total biomass of both sardinella species (*Sardinella spp.*) is available from *Dr. F. Nansen* surveys. Geographical distribution of pelagic biomass from all surveys is reported for three standard regions (e.g. Strømme et al., 1986; FAO, 2000): Northern (6°-9°S), Central (9°-13°S) and Southern (13°-17°15'S), see Figure 1.

Environmental data are collected onboard *Dr. F. Nansen* as well. Vertical profiles of temperature, salinity and oxygen are obtained with a Seabird 911+ CTD unit. In this paper, we confine our analysis to the two first two parameters. The CTD sensors are laboratory calibrated on regular basis at the Institute of Marine Research in Bergen, an institution which operates the vessel. Control measurements of salinity are conducted onboard by means of a Guildline Portasal salinometer. The typical reported standard errors of salinity are in the range of 0.006 to 0.008. Spare sensors are carried onboard for replacement should the control measurements detect deviations from these standards.

Systematic data on ocean currents are available since 2005. The currents are recorded continuously underway using a vessel-mounted Acoustic Doppler Current Profiler (ADCP), a 150 kHz phased-array Ocean Surveyor ADCP unit (Teledyne RD Instruments). The system setup and calibration was carried out in 2005 by the RDI service. Accurate navigation reference is provided by means of a Seapath 200 DGPS system. The vertical bin size to produce a single current estimate was set to 3 m; the topmost bin depth was 16 m. Tests for

misalignment angle error (Osiński, 2000) performed on the datasets used in this analysis did not indicate a time drift from the calibrated settings.

Altimetric data have been provided by AVISO (<http://www.jason.oceanobs.com/>). We used global merged maps of sea level anomalies (DT-MSLA) with grid resolution of $1/4^\circ \times 1/4^\circ$, combined from two satellite missions: TOPEX/Poseidon or Jason-1 and ERS-1/2 or Envisat (Anonymous, 2006). These maps contain the variability of SSH defined relative to the geoid and spatial changes associated to steady currents. The use of multiple satellites assures resolution of mesoscale features at scales of 100 to 300 km

(http://www.jason.oceanobs.com/html/alti/multi_sat_uk.html). From these maps, we extracted grid nodes located nearest to the African continent between Cape Lopez, Gabon (2°S) and Namibe, Angola (15°S) and spanning the period January 1993 to September 2006. Based on the extracted data, latitude-time diagrams (also known as Hovmöller diagrams) were constructed to detect propagations of SSH signals along the continental boundary. (See Chelton and Schlax, 1996; Schouten et al., 2005; Lazar et al., 2006 for other examples of use of this presentation method). The time step between two consecutive MSLA maps was one week. The mean seasonal cycle of SSH and its RMS were computed by the respective statistical moments at each extracted grid node over the corresponding weeks between 1993 and 2006, see Figure 2.

4. Results

4.1 Oceanographic regimes during the high and low SSH periods along the Angolan coast.

4.1.1 The Propagation of SSH signal along the Angola's coast

To demonstrate the annual evolution of the sea level, we derived the seasonal cycle of SSH by averaging the merged altimetric dataset over the corresponding weeks within the period 1993-2006. The evolution nearest to the African continent between Gabon to southern Angola (2° - 15°S) is shown by means of a latitude-time diagram (Figure 2a). The diagonal shapes of the SSH signal in the latitude-time space are indicative of poleward propagation of coastally-trapped Kelvin-like waves (Schouten et al., 2005). Four such propagations can be clearly identified: D1 – high SSH peak in February-March, U1- low SSH peak in

June-August, D2 – high SSH peak in October-November and U2 – a weak peak of low SSH in December-January. The expression of the poleward propagation vanishes between 12°-13°S. This latitude coincides with the rapid change of the slope of the shelf bathymetry at Baía Farta; see Figure 1. The intensity and persistence period of the SSH season changes sharply poleward of 9°S. Note that this latitude also marks the presence of the bathymetric barrier across the Angolan shelf located just south of Luanda (see Figure 1). The coincidence of strong SSH gradients between 8°-9°S with the location of this barrier suggests for geographically fixed differences in steric responses of the water column between the northern Ambriz Upwelling Area (AUA) and a more southerly located Rio Longo Upwelling Area (RLUA; see Section 2). The mean annual cycle, shown in Figure 2a, represents the average and hence smoothed image of the SSH propagations along the Angolan coast. For a comparison, we also included a diagram of SSH propagations during a specific year, 2006 (Figure 2b). The SSH gradient at 9°S is in this case clearly manifested. The outbreak of high SSH signal propagation towards the RLUA occurs in mid March, about two weeks after the high SSH front reaches first the AUA region. Note that the transition from the high to low SSH period also takes place sooner over the AUA than over RLUA.

The sea level changes along the Angolan coast are highly correlated to sea surface temperature (SST). This issue has not been a part of this analysis, but has been studied in depth by other authors (Verstraete, 1992; Hardman-Mountford et al., 2003; Florenchie et al., 2004).

In the next two paragraphs, based on the survey data, we describe oceanographic conditions, corresponding to the periods of the first annual high and low SSH propagations.

4.1.2 Water mass structure during the main high and low SSH seasons

Surveys with *Dr. F. Nansen* 1994-2006 hit the peak of high SSH (D1) during austral summer and low SSH (U1) in winter. Composite TS diagrams derived from all CTD casts 1994-2006, collected at Station A (see Figure 1) are shown in Figure 3. During summer (D1 propagation; see Figure 2), the upper layer consists of Equatorial Water (EW; Wauthy, 1977) with the temperature range 28°-30°C and salinity below 35. Just below the thermocline, salinity reaches a maximum, forming a water mass termed Salinity Maximum Water (SMW),

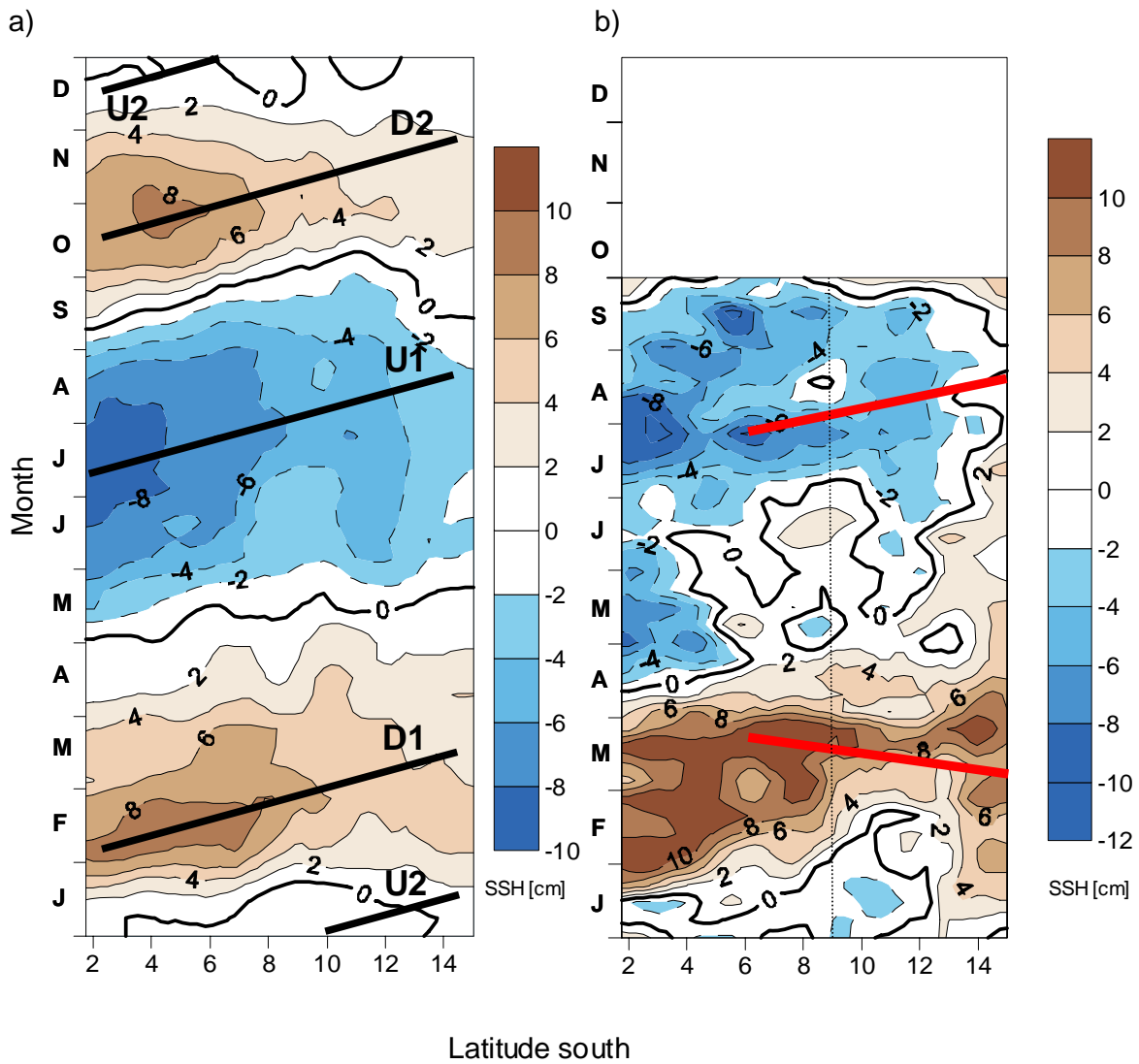


Figure 2. Latitude-time diagrams depicting poleward SSH propagations from Gabon to southern Angola (2° - 15° S): a) the mean distribution 1993-2006, b) the patterns during 2006 (January-October). The slanted black lines denote peaks of the seasonal propagations: D1 – main downwelling, U1 – main upwelling, D2 – secondary downwelling, D2 – secondary upwelling. The red lines denote the meridional track (in latitude-time coordinates) of *Dr. F. Nansen* surveys in 2006.

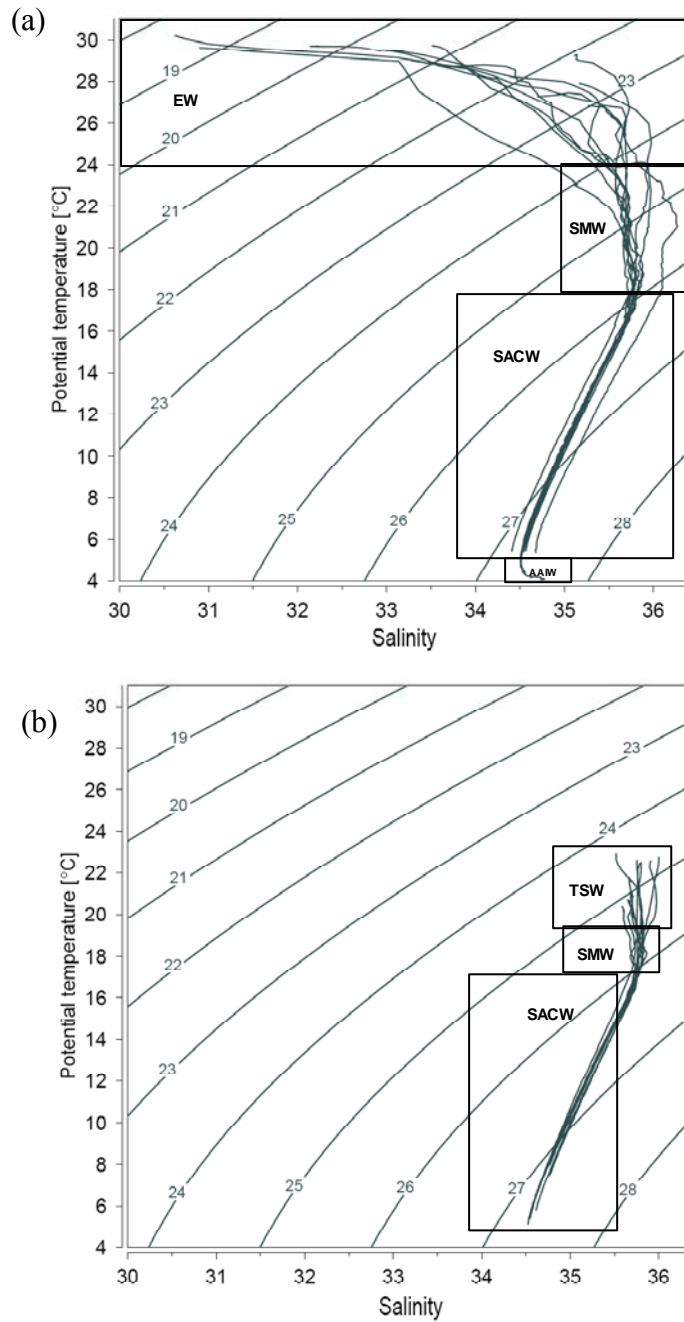


Figure 3. TS diagram from CTD casts nearest to Station A (see Figure 1 for the location) based on the 1995-2006 surveys with *Dr. F. Nansen*: (a) March/April surveys, (b) July/August surveys. Water masses: EW = Equatorial Water (Wauthy, 1997); TSW = Tropical Surface Water, SMW = Salinity Maximum Water; SACW = South Atlantic Central Water, AAIW = Antarctic Intermediate Water.

characteristic to the tropical Atlantic (Stramma et al., 2005). Below SMW, both the temperature and salinity maintain a linear relationship, an indicative of South Atlantic Central Water. This subsurface water mass is characterized by low-oxygen and high-nutrient content (Stramma and Schott, 1999), and is the source of high productivity near the coasts of Africa due to upwelling related processes (Hagen, 2001). Occasionally, CTD profiles on *Dr. F. Nansen* are conducted below 700 m hitting the layer of Antarctic Intermediate Water (AAIW), characterized by a constant temperature of a 4°C and salinity increasing with the depth. At Location A, a cast below 700 m was conducted only once in March 1998 and for this reason the AAIW layer is present in the summer diagram (Figure 3a) but absent in winter (Figure 3b). As it is evident from Figure 3, the seasonality of the water mass composition is confined to the upper layer. During winter (U1 propagation; see Figure 2), the EW layer is replaced by Tropical Surface Water (TSW; Stramma and Schott, 1999) characterized by salinity above 35.5, constant through the water column, and temperature of about 22°C at the surface, decreasing with depth to about 18°C at the top of the SMW layer. Note also a much larger year-to-year variance of the surface water masses during austral summers than winters.

Intrusions of the low salinity Equatorial Water along the coast of southeastern Atlantic from the Bay of Biafra and Congo River take place twice a year (Dessier and Donguy, 1994). The surveys with *Dr. F. Nansen* capture only the first intrusion peak (D1). A fixed station observations (Berrit and Dias, 1977) confirm that the intrusions occur semiannually, synchronous with the high SSH seasons D1 and D2, and affect the entire tropical shelf of Angola as far as to Lobito (12°20'S).

4.1.3 Vertical structure of the water column during the high and low SSH seasons.

In order to demonstrate contrasts between vertical temperature distributions during high and low SSH seasons, we selected sections occupied with *Dr. F. Nansen* in March 1996 and in the preceding August 1995 (Figure 4). Both sections highlight a change in the vertical structure at about 80 nautical miles (150 km) offshore, coinciding with the first baroclinic Rossby radius of deformation (Chelton et al., 1998). Offshore of this distance, the water column maintains the same vertical structure all year round. Inshore, the depth thermocline depth varies seasonally. During March (high SSH period, D1) the thermocline is depressed to about 50 m and isotherms slope down indicating a surface intensified poleward geostrophic current. This suggests a signature of a downwelling Kelvin-like wave, similar to

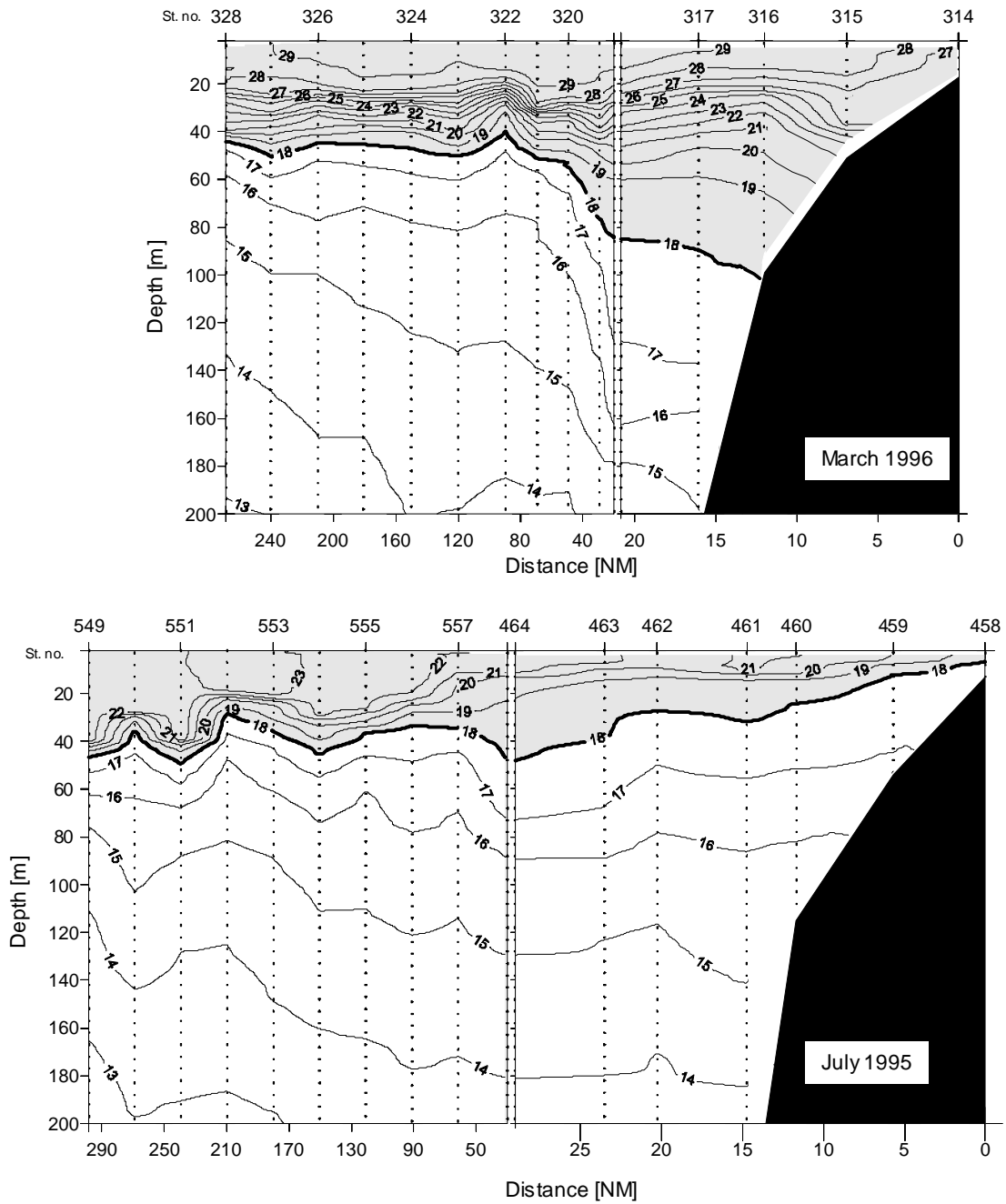


Figure 4. Sections of temperature off Pta. das Palmerinhas, representing conditions characteristic to high (March 1996) and low (July 1995) SSH propagations. The isotherm step by 1°C.

that observed off the east coast of the eastern Pacific Ocean during El Niños (Huyer et al., 2002). Above this deep thermocline, conditions are oligotrophic and the top water column is occupied by the highly stable layer of EW (Figure 2a).

In August (low SSH season, U1), the isotherms slope upwards towards the coast. Near the coast the thermocline is raised to less than 20 m deep, and the nutrient-rich subsurface SACW layer is close to the surface. The sloping upward isotherms are typically associated with a wind-driven upwelling. However, in this case wind is very low (not shown). The elevation of the thermocline is thus not maintained by the Ekman transport but has isostenic origin, similar to the tropical upwelling observed in the Gulf of Guinea (Houghton, 1976; Bakun, 1978). According to Picaut's (1983) interpretation of historical temperature data along the southeastern Atlantic coast, during austral winters upwelling Kelvin waves propagate poleward to 13°S, thus increasing the shoreward tilt of the thermocline over entire area of the tropical Angolan shelf. In accordance with the above view, the section from August 1995 (Figure 4b) may represent a temperature signature of an upwelling Kelvin-like wave. However, based on modeling results, Yamagata and Iizuka (1995) argue that coastal region off Angola is permanently cool and these conditions are only perturbed by the downwelling Kelvin waves and the associated warm water intrusions. The near-surface presence of the nutrient-rich SACW makes the tropical shelf of Angola very productive area during the low SSH periods, notwithstanding the absence of a strong upwelling favorable wind. As noted by Longhurst (1993), replenishment of the surface waters in nutrients is driven under these conditions by low energy transient mixing processes such as day-night breeze, internal waves or tidal currents and motions over the shallow water. This suggests that the highest productivity may be highly localized, confined to the inshore shallow areas and bathymetric thresholds such as the shallow bank located off Quicombo (see Figure 1)

4.1.4 Coastal currents during the high and low SSH periods in 2006.

ADCP currents were measured by means of a vessel-mounted during the first high (D1) and low (U1) SSH propagations in 2006. The meridional trace of the *Dr. F. Nansen* track in the latitude-time plot during March (Figure 2b) indicates that the current data pertain to a period of a rapid raise in SSH just south of Luanda. The currents measured in the latitude range 9°-11°S at the depth 26 m during this period are shown in Figure 5a. A strong poleward

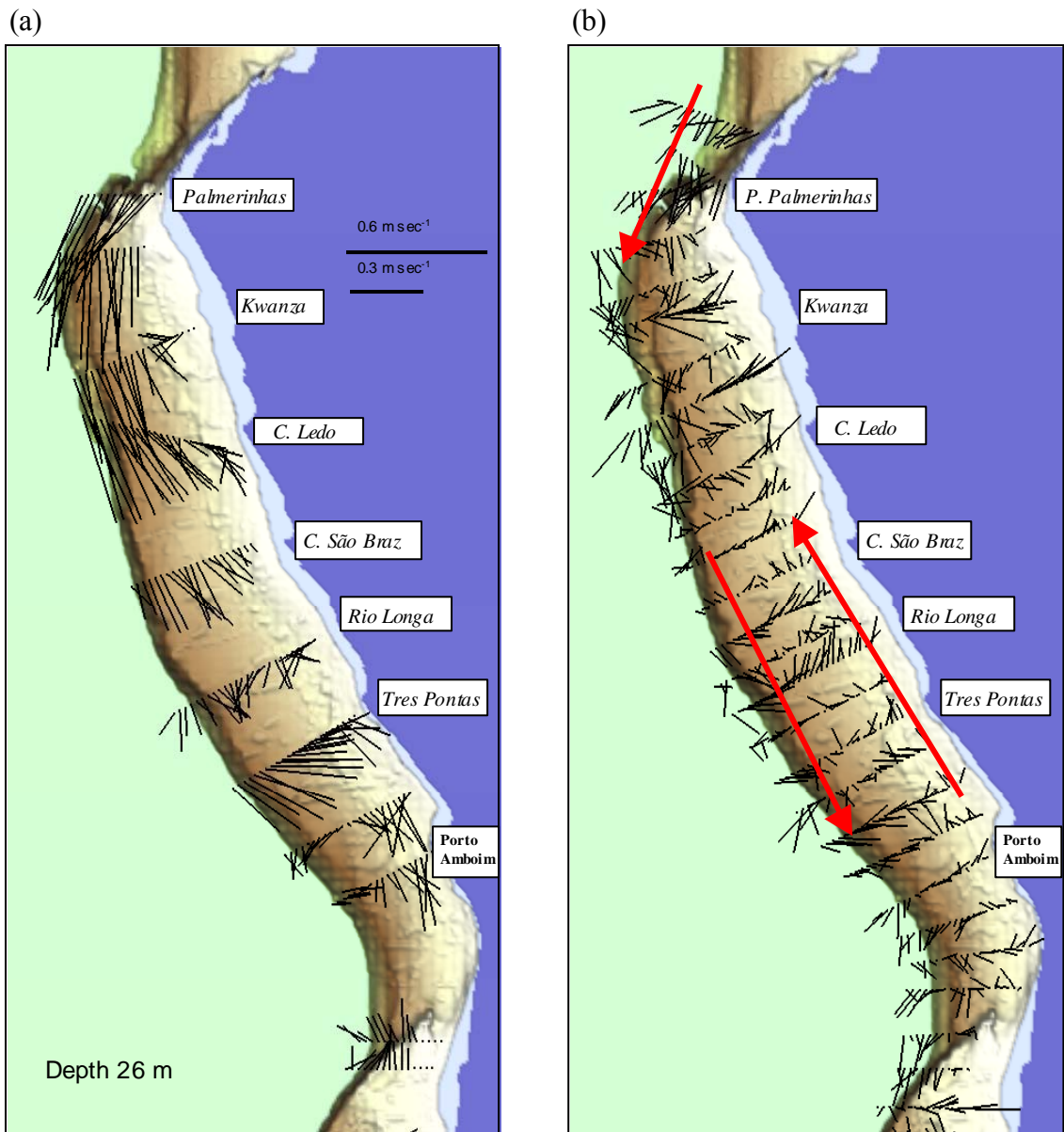


Figure 5. Distribution of ADCP-derived currents at depth 26 m between Luanda and Quicombo in 2006: a) the March (high SSH) and b) August (low SSH) conditions.

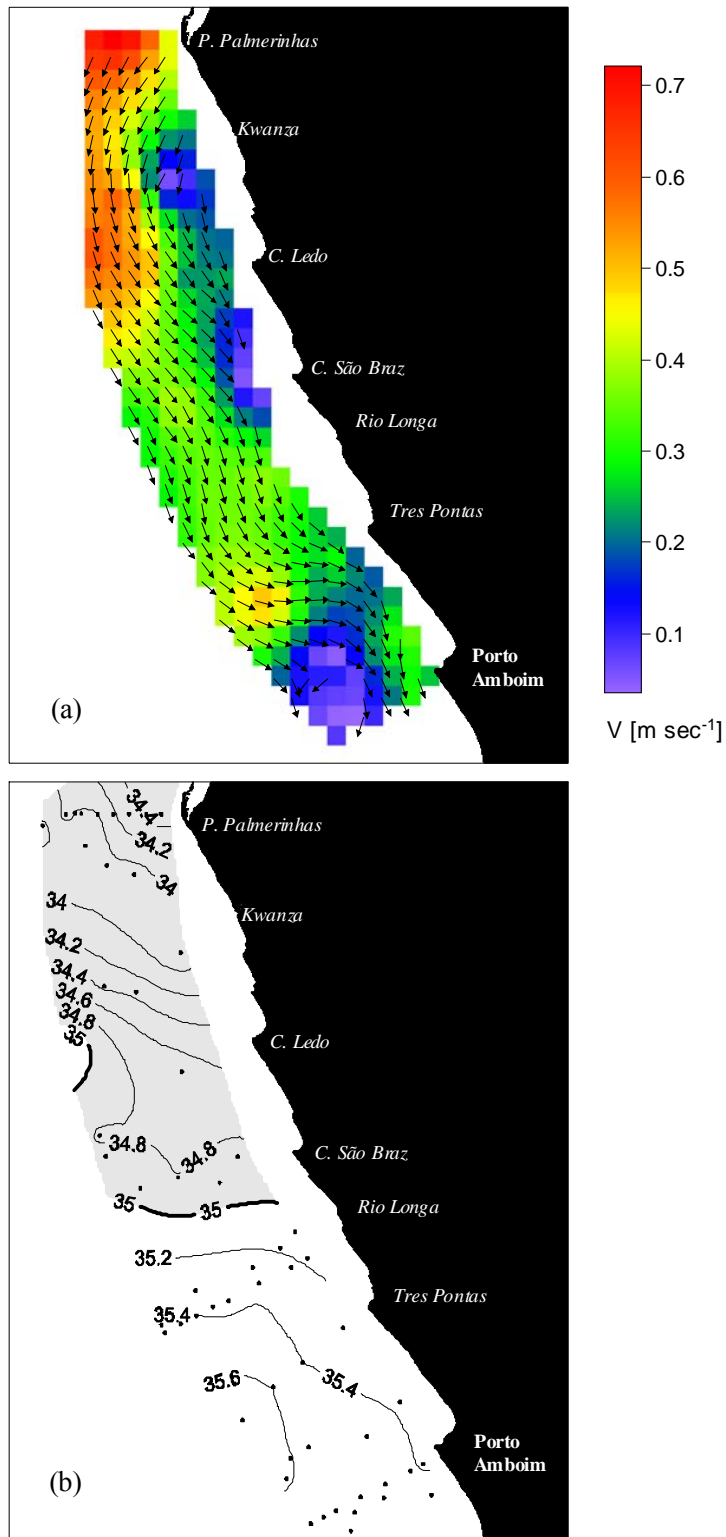


Figure 6. Current (a) at 26 m and salinity at 30 m (b) between Pta. das Palmerinhas and Porto Amboim in March 2006. The vectors denote direction only, magnitude of the current given by the color scale.

current follows the topography. A simultaneous acceleration of the poleward flow with rapid sea level rise is suggestive of a propagating Kelvin wave. Maximum current speed ($> 0.6 \text{ m sec}^{-1}$) is observed off Palmerinhas. This strong flow continues over the outer shelf to Kwanza and Cabo Ledo. Inshore at those two locations the current is weaker. At Tres Pontes there is a shoreward intensification. At Porto Amboim the inshore current intensifies above 0.2 m sec^{-1} . There is an indication of a cyclonic eddy trapped by the indentation of the shelf south of Porto Amboim. To reduce the noise, we interpolated the current data by means of ordinary kriging (Isaaks and Srivastava, 1989). The result is shown in Figure 6a. The eddy off Porto Amboim is now evident. We see that the current co-varies with the salinity distribution: in the north the flow is alongshelf while isohalines assume positions perpendicular to the coast; in the south, as the current forms an inshore meander, the isohalines assume alongshore orientation. As the current speed decreases in the center of the eddy, the salinity distribution displays a minimum ($S=35.6$), an indication Ekman suction at this location. The co-varying patterns of current and salinity increase the confidence that the observed flow resembles a real circulation feature, and not an alias from spatial undersampling of high frequency current fluctuations. A sequence of hydrographic sections between Kwanza and Port Amboim (not shown) revealed that the inshore amplified current off Porto Amboim carried a denser thermocline water outcropped to the surface between Cabo São Braz and Cabo Tres Pontas.

The currents observed in July-August 2006 (U1) are shown in Figure 5b. The current speed is lower from that observed during the outburst of the poleward jet current during March: $0.1\text{-}0.2$ vs. $0.4\text{-}0.6 \text{ m sec}^{-1}$. The results are much noisier compared to March. We do not attribute this increase of the noise to an instrumental error, because the same instrumentation, quality assurance and processing methods were applied to the ADCP data from both surveys. Rather, we attribute it to an alias due to a higher energy of the observed current in the subinertial frequency range during the low SSH season. In spite of the noise, the large-scale flow patterns can be identified. In contrast to March, the current displays little meridional gradient, but is strongly stratified across the shelf. A poleward flow dominates offshore waters over the shelf break and continental slope while in the shallow waters the current is equatorward. The current speed is much lower than in March, in the range of $0.05 - 0.2 \text{ m sec}^{-1}$.

Vertical sections of the meridional currents at Rio Longo are compared in Figure 7. In March (Figure 7a), the surface intensified and vertically-sheared poleward flow is evident. The layer with current velocity exceeding 0.1 m sec^{-1} extends to 50 m depth. The core of the flow is

found near the shelf break. The structure of this flow closely resembles currents observed in the eastern Pacific during the 1997-1998 ENSO (Kosro, 2002). An equatorward undercurrent appears below the shelf break. The core of this flow ($V=0.1 - 0.2 \text{ m sec}^{-1}$) is located below 150 m. The July-August distribution (Figure 7d) reveals a much weaker current oriented equatorward over the shelf and poleward offshore of the shelf break. The current is vertically uniform, in contrast to the March case, which indicates a strong vertical velocity shear, hence enhanced mixing. A detailed vertical profile of velocity shear (not shown) indicated that a strongest mixing occurred at the base of the thermocline, at about 50 m depth.

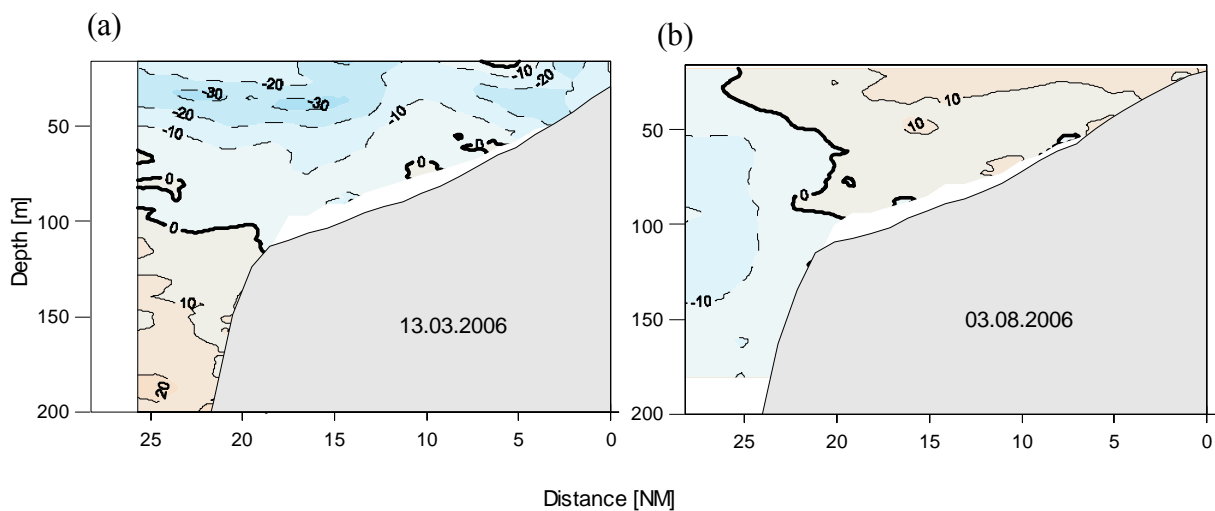


Figure 7. Vertical distribution of meridional current off Rio Longo during March (a) and August (b) 2006. Velocity in meters $\times 10^2$. Negative (positive) velocities denote poleward (equatorward) current.

4.2 The Correspondence High and low SSH conditions and distribution of sardinellas.

4.2.1 Features of the seasonal sardinella aggregations

A map of fish distribution derived from acoustic surveys reflect both behavioral and biotic factors of the true fish distribution, as well as biases related to circadian variation, avoidance, species identification or detection limits (Fréon and Misund, 1999). For this reason, it is not always simple, to single out from a survey-derived map those elements, which indicate

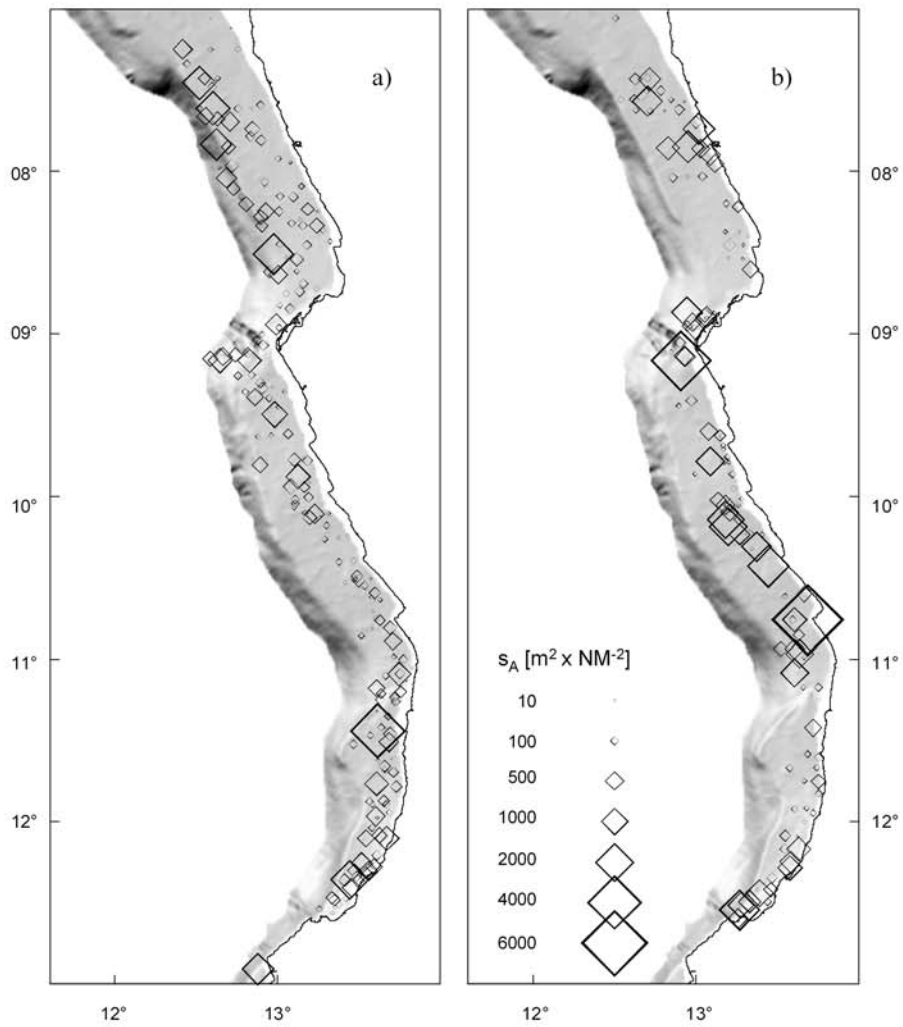


Figure 8. Distribution of acoustic abundance of sardinella: a) August 1995 (low SSH), and b) March 1996 (high SSH).

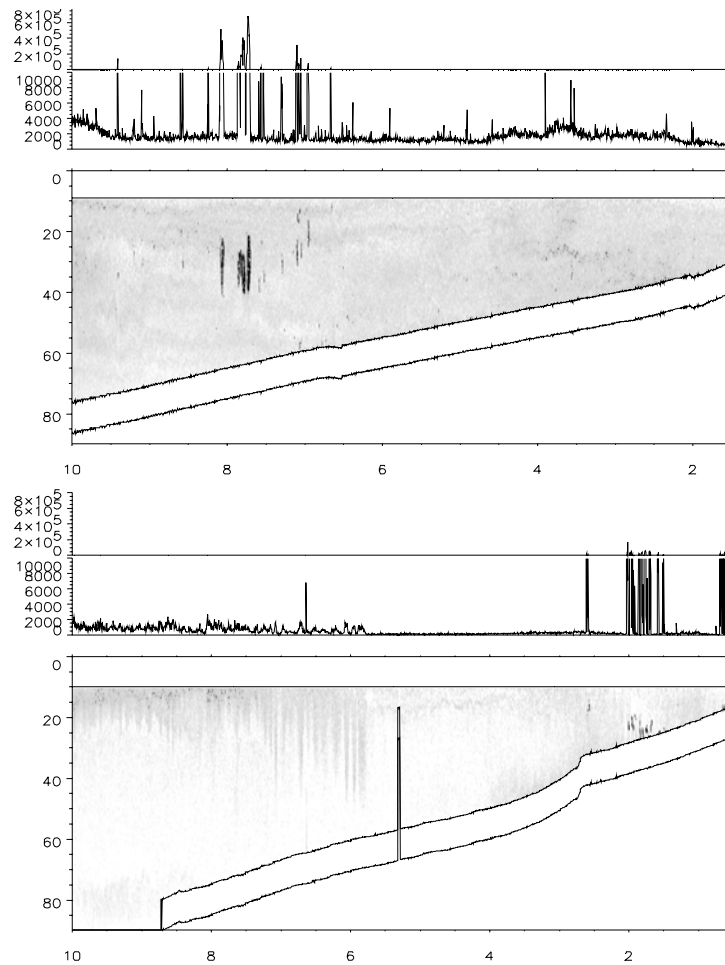


Figure 9. Sound backscattering conditions observed along the innermost (10 nautical miles) sections of acoustic transects, in (a) March 1998, and (b) August 1998. Each figure consists of two graphs. The bottom image represents a pelagic echogram of the topmost 90m of the water column, with depth displayed along the vertical axis and distance offshore along the horizontal axis. The graph above displays the s_A -values integrated for each image column separately. The scale on the upper graphs is broken into two, separately scaled areas; the lower area displays ping-based s_A -values $< 10^4$, and the upper area s_A -values above this threshold.

responses of fish aggregations to climatic factors. Yet, the distributions of sardinella the Angolan surveys often exhibit a high degree of correspondence to the major abiotic factors: shelf bathymetry and seasonal oceanographic regimes. In Figure 8, distributions of sardinella during the low SSH period in August 1995 (U1) and high SSH period in March 1996 (D1) are compared. In August (Figure 8a) the distribution was highly contiguous and uniformly distributed from the north to south. In March (Figure 8b), the distribution was clustered, with few large concentrations concentrated small areas off Luanda (9°S), Porto Amboim (10°30'S) and Benguela (12°30'S). Clearly the bulk of the biomass was located south of 9°S.

An example of schooling patterns of sardinella during the high and low SSH conditions is shown in Figure 9. Individual pings have been integrated with respect to depth and were displayed on top of the backscatter images as a function of the area backscattering coefficient s_A with distance offshore. In March 1998 (D1, Figure 9a) very few sardinella schools were found, but those that were seen were very large. The horizontal extent of some continuous aggregations along the survey track reached about 0.2 nautical mile. The largest aggregations were observed over the deep water at the thermocline depth. In August 1998 (U1, Figure 9b) sardinella schools were seen along the entire tropical shelf, occupying the region of the surfacing thermocline in a depth range 30-45m. More schools, and larger in size were observed during daytime than at night, when part of the stock tended to disperse and offshore.

4.2.2 Correspondence between the meridional distribution of sardinella biomass and seasonal propagations of SSH

Evolution of sardinella biomass from 1994 to 1998 in the three geographical regions: Northern (6°-9°S), Central (9°-13°S) and Southern (13°-17°15'S) is shown in Figure 10. Each diagram represents one survey from 1994 until 1998, bottom-up. The results during austral summer are show in the gray color; those during winter are shown in white. The symbols next to the diagrams denote survey year, start month and a symbol of the corresponding SSH propagation from Figure 2a. For instance, 98-03 D1 denotes a survey starting in March 1998 during the first seasonal high peak of SSH. Data gaps are marked with the crosses: Southern region was not covered before the winter survey in 1996 and there was no biomass estimate during the summer 1997.

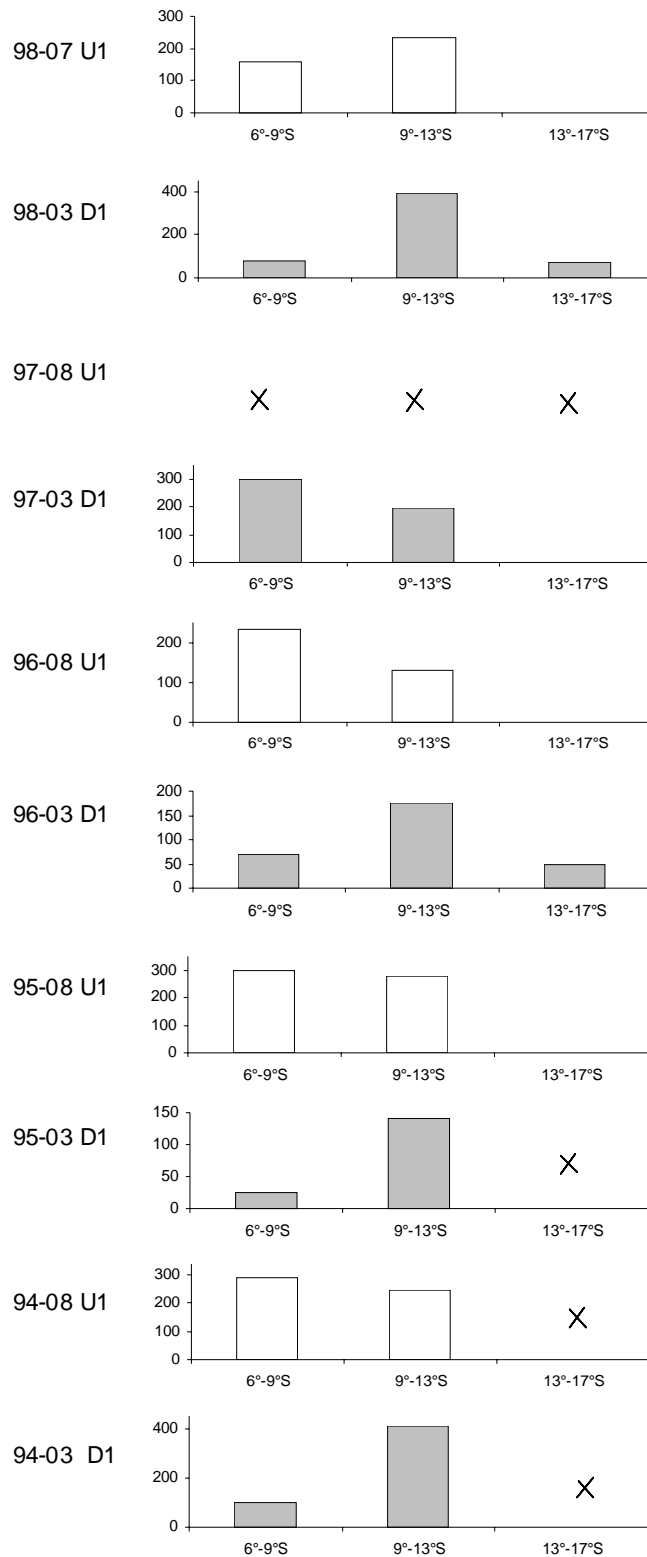


Figure 10. Distribution of acoustically derived biomass of sardinellas in three regions along the coast, 1994-1996. Survey symbols given in the left. The summer surveys (high SSH) shaded. The crosses denote not sampled data.

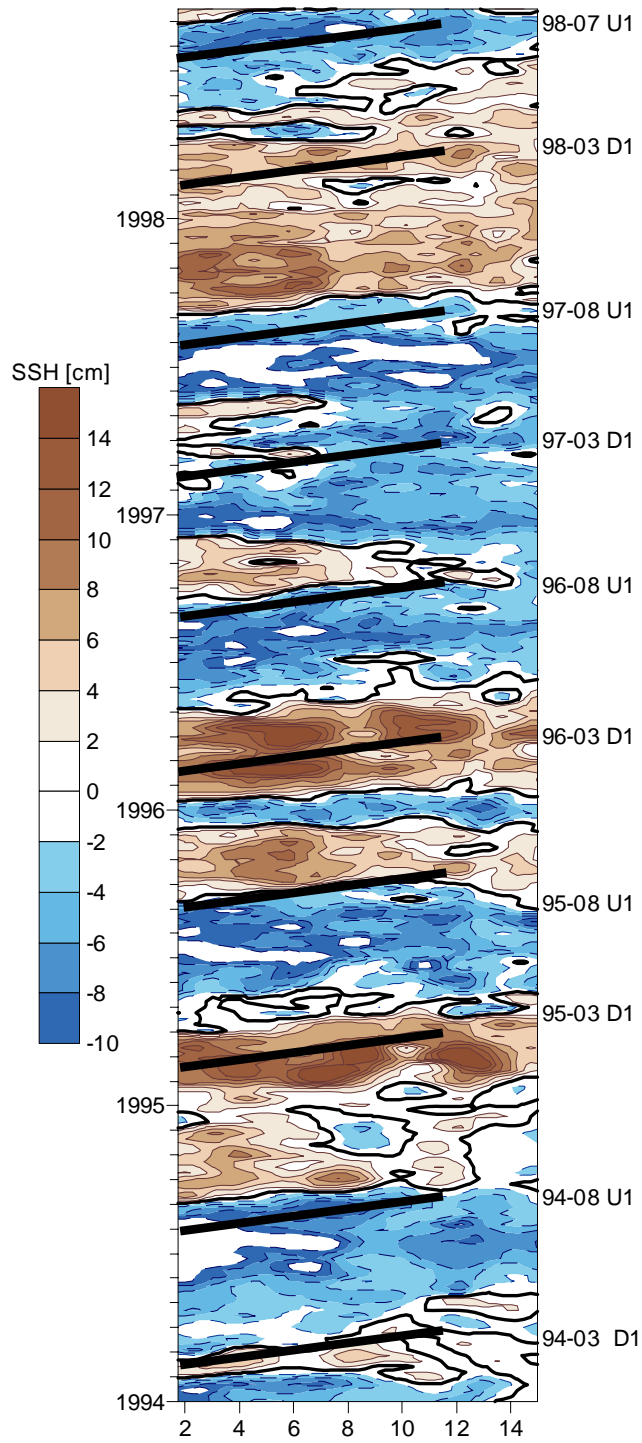


Figure 11. Latitude-time diagram of the SSH propagations between Gabon and southern Angola 1994-1998. Horizontal and vertical axes denote latitude in degrees, and time in months respectively. The slanted lines denote peaks of climatological propagations. Description of surveys pertaining to those peaks given to the right.

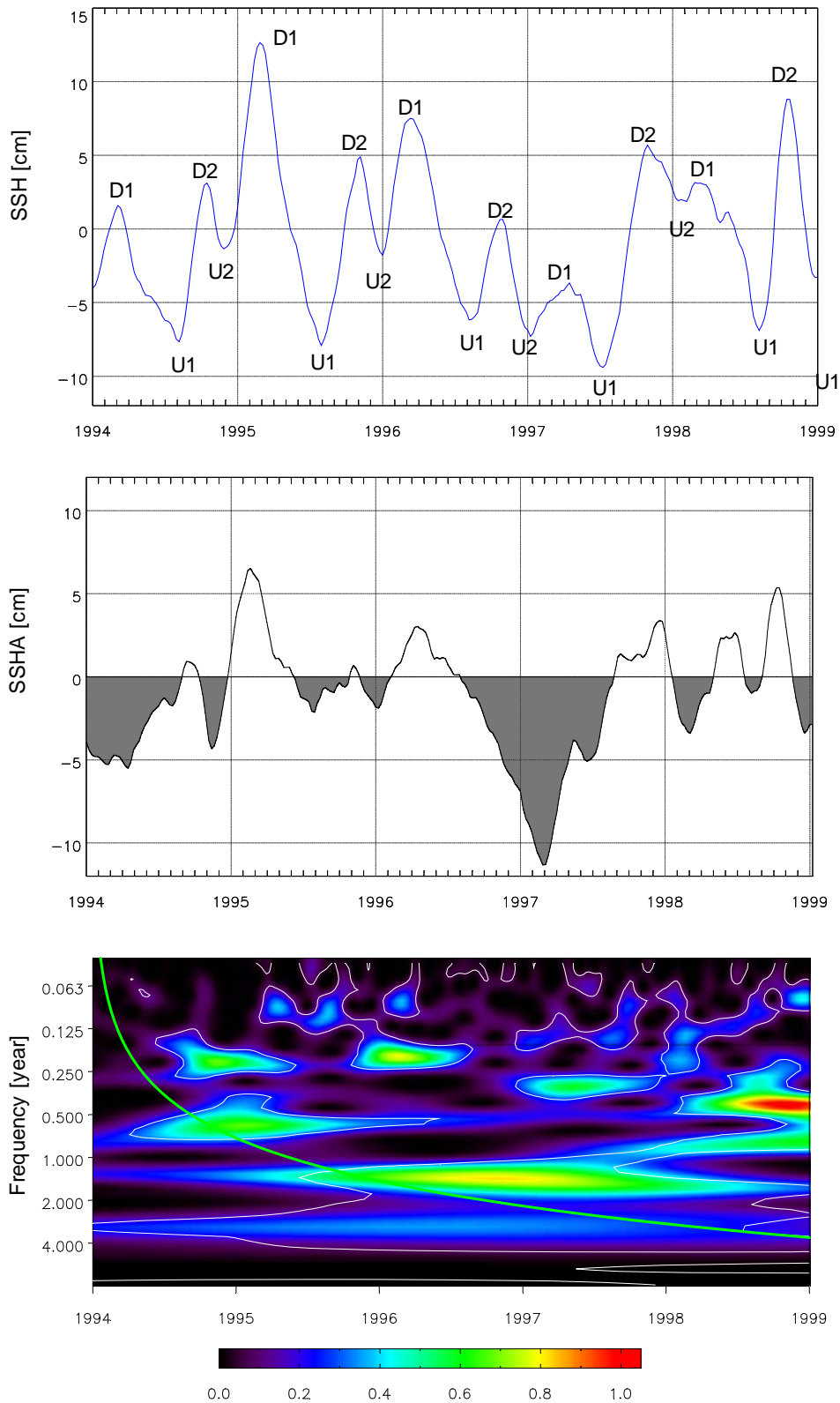


Figure 12. Evolution of SSH in the AUA region, 1994-1998 (Top), SSH anomaly (middle), wavelet transform of the SSH (bottom). The horizontal axis scaled in years and months. Symbols in the top figure denote peaks of the propagations (see Figure 2).

Figure 10 highlights the well-known seasonal distribution pattern of the sardinella stock (FAO, 2000), whereby the center of the biomass shifts toward the south during summer and reverts to the north during winter. Also note that in the cases when the biomass estimate is available for the Southern region, fish is found there during austral summer, but not in winter. These facts support the pattern of the seasonal sardinella migrations known from the literature (Da Fonseca Baptista, 1977; Boley and Fréon, 1980). However, a closer inspection of Figure 10 reveals number of anomalies from the mean seasonal pattern, most notably these three: (1) in summer 1995, the total biomass estimate is very low (95-03 D1) ; (2) the next estimate half a year later shows a threefold increase in the biomass (95-08 U1); (3) in summer 1997 (Survey 97-03 D1) the usual seasonal southward shift of the biomass was not observed.

In order to determine if the above deviations in the biomass estimates can be associated to anomalous seasonal oceanographic conditions, we investigated the evolution of SSH signal during the pertaining period 1994-1998 (Figure 11, 12 and 13). These figures convey essentially the same information but with a different degree of detail. Figure 11 displays a time-latitude diagram of SSH propagations during 1994-1998. Figure 12 presents the evolution of a mean SSH levels spatially averaged of over the AUA region (see Section 2). Three views of this time series are presented: a) absolute SSH (the data extracted from AVISO maps); b) SSH anomalies relative the long term mean 1993-2006; c) wavelet transform of the anomalies (Torrence and Compo, 1998). Figure 13 shows the same SSH series as Figure 12a, but overlaid with evolution of the total biomass in Angolan waters between 1994 and 1998.

Returning to the above listed anomalies in the biomass patterns we note the following:

1. The extremely low biomass estimated in summer 1995 coincides with the most extreme peak of anomalously high SSH (Survey 95-03 D1). This SSH anomaly manifests the strongest warm event in the southeastern Atlantic during the decade known as the 1995 Benguela Niño (Hardman-Mountford et al., 2003). Gammelsrød et al. (1998) reported extreme oceanographic conditions during this period, characterizing the high SSH regime (see Section 4.1). The very low estimates of sardinella during this period are believed to be caused by fish behavior. Sardinella was dispersed; its echo-traces difficult to separate from plankton (FAO, 2000). We also note the estimate may have been biased by the lack of the survey coverage in the

Southern region (13°-17°S). Since the poleward current associated to high SSH was presumably very strong, a large component of the stock had probably migrated away to that region and was thus unaccounted in the biomass estimate.

2. A jump in the estimated biomass from 200 to nearly 600 thousand tones observed in just four months after the 1995 Benguela Niño (Figure 13) cannot be considered to a sign of an increase in fish production. Rather, the fish dispersed during the Benguela Niño migrated northwards to the region fully covered by the survey. The aggregations returned to a highly contagious wintertime distribution patterns (see Figure 8a). Accordingly, the biomass estimate matched the levels from the previous winter (Figure 13). A similar pattern of a decline and subsequent rise of biomass estimates from acoustic surveys was reported for anchovies in the eastern Pacific during the 1997-1998 El Niño/ El Niño (Bertrand et al., 2004).
3. The summer 1997 (Survey 97-03 D1) was characterized by a strong negative SSH anomaly (Figure 12b). Handoh and Bigg (2000) describe this anomaly as a part of a 2 years long climate event. It was also the coldest event during the decade (Florenchie et al., 2004). The two-years period of the fluctuation associated with this anomaly is evident on the wavelet transform (Figure 12c). The usual downwelling SSH propagation (D1) did not take place (Figure 11). This suggests a weak or absent poleward current hence the absence of the transport mechanism stimulating the summertime migration of fish to the south. From Figure 10, Survey 97-03 D1 it is clear that indeed summer 1997 the bulk of biomass remained in the north, presumably occupying its habitat from the preceding winter (Survey 96-08 U1).

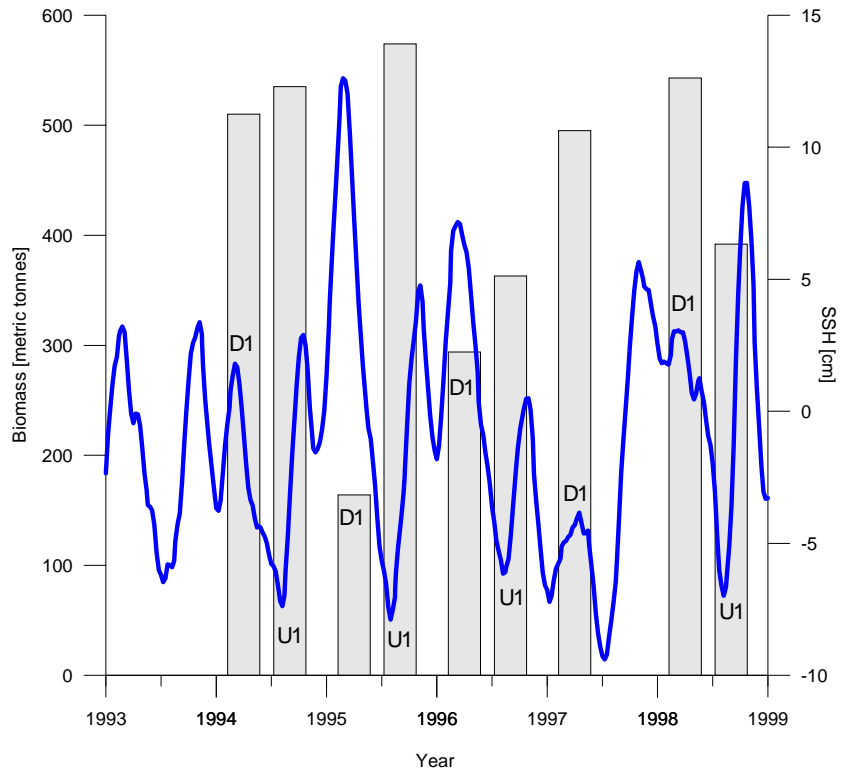


Figure 13. Seasonal trends in the sardinella biomass off Angola 1994-1998 (bars) vs. evolution of SSH in the AUC region (line). The symbols denote downwelling and upwelling propagations, see Figure 2.

5. Conclusions

Based on our analysis we can now summarize the linkages at the Angolan coast between remotely sensed Kelvin waves, oceanographic regimes determined by them and responses in the biomass sardinella detected from acoustic surveys:

1. Strong oscillations in environmental conditions in the topical sector of the Angola shelf occur on seasonal scales in connection with the semiannual cycle of coastally-trapped Kelvin waves, detectable by means of satellite altimetry.
2. An arrival of downwelling (high pressure) coastal wave in February-March is associated with a depression of the thermocline, strong stratification and intrusion of oligotrophic Equatorial Water at the surface. The coastal flow is poleward, vertically sheared and strong ($0.3-0.6 \text{ m sec}^{-1}$). The vertical stratification, depth of the thermocline and thickness of the oligotrophic surface layer exhibit meridional gradients. These conditions in the north are less favorable for primary production than in the south
3. During the upwelling season in July-August, the thermocline rises close to the surface despite of the absence an upwelling favorable wind. The pool of nutrients sourced from South Atlantic Central Water (SACW) is present just below the shallow thermocline. Replenishment of nutrients in the surface layer is determined by topographic detail and intermittent small scale processes. Environmental conditions are uniform meridionally, but exhibit an inshore-offshore zonation.
4. The seasonal oscillations in environmental conditions yield sharp changes to favorable habitats of small pelagic fish. During downwelling periods, conditions for spawning and grazing are poor. The strong poleward flow and more favorable environmental conditions in the south stimulate fish to undertake seasonal migrations. During the upwelling season, the strongest mixing and productivity is observed in the inshore waters. Conditions for spawning and grazing are equally favorable in the north and south. However, since the remotely-forced upwelling signal propagates from an equatorial source, favorable habitats for fish emerge first in the north.

5. Acoustic surveys appear to detect responses of sardinella aggregations to the seasonal oscillations in environmental conditions. During downwelling periods, fish is dispersed across the water column or is found in few large schools with no particular spatial organization. The bulk of the biomass migrates to the south. During upwelling seasons, distributions are highly contagious from the north to south and located predominantly in the vicinity of the coast and shallow topographic features.

6. Seasonal shifts in geographical distribution of the sardinella stock and hence fish availability to local fisheries are modulated by anomalous climatic events in the southeastern Atlantic. The extreme warm event in February-March 1995, caused dispersion of the stock making it inaccessible to acoustic sampling. In the wake of this event, the estimated biomass was the largest in the decade, presumably due to massive advection and migration of fish with the poleward current. The extreme cold event in February-March 1997 inhibited the seasonal fish migration, seemingly due to an absence of this current.

7. Sardinellas are clearly well adapted to seasonally varying productive and unproductive regimes. Therefore dramatic collapses of its biomass due to short acute climatic events of the Benguela Niño type are unlikely. However, these events can significantly modulate the seasonal aggregation and migration patterns and fish less available local fishermen.

6. References.

- Anonymous. (2006). SSALTO/DUACS User Handbook: (M)SLA and (M)ADT Near-Real Time and Delayed Time Products. SALP, CLS-DOS-NT-0.6.034, [http://www.jason.oceanobs.com/documents/donnees/duacs/handbook_duacs.pdf].
- Bakun, A. (1978). Guinea Current upwelling. *Nature* **271**:147-150.
- Bakun, A. (1996). Patterns in the Ocean: ocean processes and marine population dynamics. Calif. Sea Grant College Syst. Univ of Calif, La Jolla. 323 pp.
- Berrit, G.R. (1976). Les eaux froides côtières du Gabon à L'Angola sont-elles dues à un upwelling d'Ekman. *Cah. ORSTOM, sér. Océanogr.* **14**:473-478.
- Berrit, G.R. and Dias, C.A. (1977). Hydroclimatologie des Régions Côtières de L'Angola. *Cah. ORSTOM, sér. Océanogr.* **15**:181-196.
- Bertrand, A., Seguera, M., Gutiérrez, M. and Vásquez, L. (2004). From small-scale habitat loopholes to decadal cycles: a habitat-based hypothesis explaining fluctuation in pelagic fish populations off Peru. *FISH and FISHERIES* **5**:296-316.
- Bianchi, G. (1992). Demersal assemblages of the continental shelf and upper slope of Angola. *Mar. Ecol. Prog. Ser.* **81**:101-120.
- Binet, D., Gobert, B. and Maloueki, L. (2001). El Niño-like warm events in the Eastern Atlantic (6°N, 20°S) and fish availability from Congo to Angola (1964-1999). *Aquat. Living Resour.* **14**:99-113.
- Boley, T. and Fréon, P. (1980). Coastal Pelagic Resources. In The Fish Resources of the Eastern Central Atlantic. Part One: The Resources of the Gulf of Guinea from Angola to Mauritania. FAO Fisheries Technical Paper No. 186.1. Troadec, J. P. and Garcia, S. (Eds.). Rome, FAO 13-76.
- Chelton, D.B., deSzoeki, M.G., Schlax, M.G., Naggar, K.E. and Siwetz, N. (1998). Geographical variability of the first-baroclinic Rossby radius of deformation. *J. Phys. Oceanogr.* **28**:433-460.
- Chelton, D.B. and Schlax, M.G. (1996). Global observations of oceanic Rossby waves. *Science* **272**:234-237.
- Da Fonseca Baptista, S.R. (1977). The distribution and movements of the sardinellas (*Sardinella aurita* VAL and *Sardinella eba* VAL) off the Angolan coast. *Coll. scient. Pap. int. Comm. SE. Atl. Fish.* **4**:21-24.
- Dessier, A. and Donguy, J.R. (1994). The surface salinity in the tropical Atlantic between 10°S and 30°N-seasonal and interannual variations (1977-1989). *Deep-Sea Res. I* **41**:81-100.

- FAO. (1979). Report of the Ad Hoc Working Group on Sardinella Stocks from Congo to Southern Angola. CECAF/ECAF Series - 80/20
[\[http://www.fao.org/DOCREP/003/N8488E/N8488E00.HTM\]](http://www.fao.org/DOCREP/003/N8488E/N8488E00.HTM).
- FAO (2000) Report of the Workshop on the Small Pelagic Resources of Angola, Congo and Gabon. FAO Fish Rep. 618, FIRM/SAFR/R618, 149 pp.
[\[ftp://ftp.fao.org/docrep/fao/007/x8118e\]](ftp://ftp.fao.org/docrep/fao/007/x8118e)
- Florenchie, P., Lutjenharms, J.R.E., Reason, C.J.C., Masson, S. and Rouault, M. (2003). The source of Benguela Niños in the South Atlantic Ocean. *Geophys. Res. Lett.* **30**:1505 (doi:1029/2003GLO17172).
- Florenchie, P., Reason, C.J.C., Lutjenharms, J.R.E. and Rouault, M. (2004). Evolution of interannual warm and cold events in the southeast Atlantic Ocean. *J. Climate* **17**:2318-2334.
- Foote, K.G., Knudsen, H.P., Korneliussen, R.J., Nordbø, P.E. and Røang, K. (1992). Post-processing system for echo sounder data. *J. acoust. Soc. Am.* **91**:1983-1989.
- Foote, K.G., Knudsen, H.P., Vestnes, D.N., MacLennan, D.N. and Simmonds, E.J. (1987). Calibration of acoustic instruments for fish density estimation: a practical guide. *ICES Coop. Res. Rep. No.* **144**:1-69.
- Fréon, P. and Misund, O.A. (1999). Dynamics of Pelagic Fish Distribution and Behaviour: Effects on Fisheries and Stock Assessment. Fishing News Books. 348
- Gammelsrød, C.H., Bartholomae, C.H., Boyer, D.C., Filipe, V.L. and O'Toole, M.J. (1998). Intrusion of warm surface waters along the Angolan-Namibian coast in February-March 1995: The 1995 Benguela Niño. *S. Afr. J. mar. Sci.* **19**:41-56.
- Hagen, E. (2001). Northwest African upwelling scenario. *Oceanologica Acta* **24 (Supplement)**:113-128.
- Handoh, I.C. and Bigg, G. (2000). A self-sustaining climate mode in the tropical Atlantic, 1995-1997: observation and modeling. *Q. J. R. Meteorol. Soc.* **126**:807-821.
- Hardman-Mountford, N.J., Richardson, A.J., Agenbag, J.J., Hagen, E., Nykjaer, L., Shillington, F.A. and Villacastin, C. (2003). Ocean climate of the South East Atlantic observed from satellite data and wind models. *Prog. Oceanogr.* **59**:181-221.
- Houghton, R.W. (1976). Circulation and hydrographic structure over the Ghana continental shelf during the 1974 upwelling. *J. Phys. Oceanogr.* **6**:909-924.
- Huyer, A., Smith, R.L. and Fleishbein, J. (2002). The coastal ocean off Oregon and northern California during the 1997-8 El Niño. *Prog. Oceanogr.* **54**:311-341.
- Isaaks, E.H. and Srivastava, E.H. (1989). Applied Geostatistics. New York, Oxford. Oxford University Press. 561 pp.
- Kosro, P.M. (2002). A poleward jet and equatorward undercurrent observed off Oregon and Northern California, during the 1997-98 El Niño. *Progr. Oceanogr.* **54**:343-363.

- Lazar, A., Polo, I., Arnault, S. and Mainsant, G. (2006) Kelvin waves activity in the eastern tropical Atlantic. Conference 15 Years of Progress in Radar Altimetry, 6 pp.
[\[http://earth.esa.int/workshops/venice06/participants/1263/paper_1263_lazar.pdf\]](http://earth.esa.int/workshops/venice06/participants/1263/paper_1263_lazar.pdf)
- Longhurst, A.R. (1993). Seasonal cooling and blooming in tropical oceans. *Deep-Sea Res.* **40**:2145-2165.
- MacLennan, D.N., Fernandez, P.G. and Dalen, J. (2002). A consistent approach to definitions and symbols in fisheries acoustics. *ICES J. Mar. Sci.* **59**:365-369.
- Moore, D.W., Hisard, P., McCreary Jr., J.P., Merele, J., O'Brien, J.J. and Picaut, J. (1978). Equatorial adjustment in the eastern Atlantic. *Geophys. Res. Lett.* **5**:637-640.
- Osiński, R. (2000). The misalignment angle in vessel-mounted ADCP. *Oceanologia* **42**:385-394.
- Philander, S.G. and Pacanowski, R.C. (1986). A model of the seasonal cycle in the Tropical Atlantic Ocean. *J. Geophys. Res.* **91**(C12):14192-14206.
- Picaut, J. (1983). Propagation of the seasonal upwelling in the eastern equatorial Atlantic. *J. Phys. Oceanogr.* **13**:18-37.
- Rouault, M. and Lutjeharms, J.R. (2003). Estimation of sea surface temperature around southern Africa from satellite-derived microwave observations. *S. Afr. J. Sci.* **99**:498-494.
- Sætelsdal, G., Bianchi, G. and Strømme, T. (1999) The Dr. Fridtjof Nansen Programme 1975-1993. Investigations of fishery resources in developing regions. History of the programme and review of results. FAO Fisheries Technical Paper 391. Rome, 434 pp.
[\[http://www.fao.org/DOCREP/004/X3950E/X3950E00.HTM\]](http://www.fao.org/DOCREP/004/X3950E/X3950E00.HTM)
- Schouten, M.W., Matano, R.P. and Strub, T.P. (2005). A description of the seasonal cycle of the equatorial Atlantic from altimeter data. *Deep-Sea Res. I* **52**:477-493.
- Shannon, L.V., Boyd, A.J., Brundrit, G.B. and Taunton-Clark, J. (1986). On existence of an El Niño-type phenomenon in the Benguela System. *J. Mar. Res.* **44**:495-520.
- Shannon, L.V. and Nelson, G. (1996). The Benguela: large scale features and processes and system variability. In *The south Atlantic: Present and Past Circulation*. Wefer, G., Berger, W. H., Siedler, G. and Webb, D. J. (Eds.). Berlin Heidelberg 163-210.
- Stramma, L., Hüttl, S. and Schafstall, J. (2005). Water masses and currents in the upper northeast Atlantic off northwest Africa. **110**:doi:10.1029/2005JC002939.
- Stramma, L. and Schott, F.A. (1999). The mean flow field of the tropical Atlantic Ocean. *Deep-Sea Res. II* **46**:279-303.

Strømme, T. and Sætelsdal, G. (1991). Surveys of Marine Fish Resources of Angola 1985-86 and 1989. Reports on surveys with *R/V Dr. F. Nansen*. Institute of Marine Research, Bergen, Norway.

Strømme, T., Sætelsdal, G. and Fontes Pereira, A. (1986) Report on the Surveys of Angola's Marine Fish Resources January 1985 - June 1986. FAO Corporate Document Repository, [<http://www.fao.org/WAIRDOCS/FNS/AA041E/AA041E00.HTM>]

Torrence, C. and Compo, G.P. (1998). A practical guide to wavelet analysis. *Bull. Am. Meteo. Soc.* **69**:61-78.

Verstraete, J.T. (1992). The seasonal upwellings in the Gulf of Guinea *Prog. Oceanogr.* **29**:1-60.

Wauthy, B. (1977). Révision de la Classification de Surface du Golfe de Guinée (Berrit 1961). *Cah. ORSTOM, sér. Océanogr.* **15**:279-295.

Yamagata, T. and Iizuka, S. (1995). Simulation of the tropical thermal domes in the Atlantic: A seasonal cycle. **25**:2129-2140.